IMPEDANCE SPECTROSCOPY OF MICROSTRUCTURES

ME5204 Finite Element Analysis (course project)

VYAS VEDANSHU GAURAGBHAI

Department of Mechanical Engineering,
Indian Institute of Technology Madras, Chennai - 600036, India.
me21b218@smail.iitm.ac.in

Abstract

We implement FEM for an accurate simulation of the impedance spectroscopy(IS) of polycrystalline materials. Using Finite element method(FEM), we did explicit meshing of grain and grain boundaries, then checked mesh convergence for potential which was calculated using implicit scheme with the necessary boundary conditions and then went on to obtain the current and eventually the Nyquist plots to observe the variation in impedance with frequencies. We observed that Nyquist plots give a semi-circular curve.
Keywords: Mesh, Convergence, Plots

Introduction

Impedance spectroscopy (IS) is a vital experimental technique used to characterize materials by analyzing their electrical responses. In materials science, IS is particularly useful for understanding the contributions of various microstructural features, such as grains and grain boundaries, to the overall electrical behavior of polycrystalline samples. The technique typically involves generating Nyquist plots, which provide valuable insights into resistance and capacitance characteristics. These plots allow researchers to model the material's response using equivalent circuits, facilitating the study of electrical properties and the impact of microstructure on performance.

Conventional numerical approaches, such as the finite element method (FEM), are extensively used to simulate IS. FEM provides a robust framework for solving spatio-temporal Maxwell's equations, enabling the prediction of electrical behavior across heterogeneous domains. For example, FEM has been used to investigate the influence of porosity on the electrical properties of BaTiO3 and to model current density distributions in polycrystalline materials. However, FEM-based simulations are computationally expensive, particularly when fine meshes are required to capture high-gradient regions such as grain boundaries. These limitations pose challenges for large-scale simulations or when studying complex microstructures with varying grain sizes and boundary widths.

In this study, we focus on employing FEM to simulate impedance spectroscopy for polycrystalline materials, with an emphasis on accuracy and computational efficiency. The goal is to demonstrate the application of FEM in generating IS data for microstructures with varying properties and to evaluate the computational trade-offs involved.

The rest of the report is organized as follows: Section 2 introduces the governing equations and their weak form used in FEM. Section 3 describes the discretization approach adopted in the

simulations. Section 4 presents a numerical example to illustrate the methodology and its results. Finally, Section 5 concludes the report with a summary of findings and potential future directions.

Governing Equations and Weak Form

The problem involves simulating the electrical response of a polycrystalline material using impedance spectroscopy (IS). The governing equations are derived from Maxwell's continuity equation and Ohm's law, describing the relationship between current density, electric field, and material properties. This section outlines the strong form, weak form, and boundary conditions applied to the finite element method (FEM) simulation.

Strong Form of the Problem

The differential form of Maxwell's continuity equation is given as:

$$\frac{\partial \rho}{\partial t} + \nabla \cdot \mathbf{J} = 0, \tag{1}$$

where ρ is the charge density, and $\mathbf{J}$ is the total current density.

The total current density $\mathbf{J}$ is expressed as:

$$\mathbf{J} = \mathbf{J}_c + \mathbf{J}_d, \tag{2}$$

where $\mathbf{J}_c = \sigma \mathbf{E}$ is the conduction current density, and $\mathbf{J}_d = \frac{\partial \mathbf{D}}{\partial t}$ is the displacement current density. Here, σ is the electrical conductivity, $\mathbf{E}$ is the electric field, and $\mathbf{D}$ is the electric displacement.

The electric field $\mathbf{E}$ and electric displacement $\mathbf{D}$ are related by:

$$\mathbf{E} = -\nabla \phi, \quad \mathbf{D} = \epsilon \mathbf{E}, \tag{3}$$

where ϕ is the electric potential, and ϵ is the permittivity of the material. Substituting these relations, the governing equation becomes:

$$-\nabla \cdot (\sigma \nabla \phi) + \nabla \cdot \left(\epsilon \frac{\partial (\nabla \phi)}{\partial t} \right) = 0. \tag{4}$$

Assuming constant permittivity ($\epsilon_r = 100$) and conductivity ($\sigma = 1$ S/m) for the entire domain, the equation simplifies to:

$$-\nabla \cdot (\nabla \phi) + \epsilon \frac{\partial (\nabla^2 \phi)}{\partial t} = 0. \tag{5}$$

Weak Formulation

The governing equation is transformed into its weak form to facilitate numerical solution using the finite element method (FEM). The strong form of the equation is:

$$-\nabla \cdot (\sigma \nabla \phi(x,t)) + \epsilon \frac{\partial (\nabla \cdot \nabla \phi(x,t))}{\partial t} = 0, \quad \forall x \in \Omega, \tag{6}$$

where σ is the electrical conductivity, ϵ is the permittivity, and $\phi(x,t)$ is the electric potential.

The corresponding weak form is:

$$\text{Find } \phi \in U \text{ such that } \forall \delta\phi \in V, \tag{7}$$

$$\int_\Omega \sigma \nabla \delta\phi \cdot \nabla \phi(x,t)\, d\Omega + \int_\Omega \epsilon \nabla \delta\phi \cdot \frac{\partial \nabla \phi(x,t)}{\partial t}\, d\Omega = \int_{\partial\Omega} \delta\phi\, \mathbf{n} \cdot (\sigma \nabla \phi(x,t))\, d\Gamma. \tag{8}$$

This weak form consists of: - Bilinear Term:

$$\int_\Omega \sigma \nabla \delta\phi \cdot \nabla \phi(x,t)\, d\Omega, \tag{9}$$

representing the conduction component.

- Linear Term:

$$\int_\Omega \epsilon \nabla \delta\phi \cdot \frac{\partial \nabla \phi(x,t)}{\partial t}\, d\Omega, \tag{10}$$

capturing the displacement current contribution.

- Boundary Term:

$$\int_{\partial\Omega} \delta\phi\, \mathbf{n} \cdot (\sigma \nabla \phi(x,t))\, d\Gamma, \tag{11}$$

describing the potential flux through the boundaries.

Here, U and V denote the trial and test spaces that include linear fields.

Boundary Conditions

The boundary conditions for the problem are specified as follows: 1. **Top Surface (Dirichlet Condition)**: A sinusoidal voltage is imposed:

$$\phi(x,t) = V_0 \sin(\omega t), \quad \text{on } \Gamma_{\text{top}}. \tag{12}$$

2. **Bottom Surface (Dirichlet Condition)**: The potential is fixed at zero:

$$\phi(x,t) = 0, \quad \text{on } \Gamma_{\text{bottom}}. \tag{13}$$

3. **Side Boundaries (Neumann Condition)**: Zero flux is assumed:

$$\mathbf{n} \cdot \nabla \phi(x,t) = 0, \quad \text{on } \Gamma_{\text{sides}}, \tag{14}$$

where $\mathbf{n}$ is the outward normal vector.

Material Properties and Simulation Parameters

The material properties and parameters used in the simulation are:

- Permittivity: $\epsilon = 100$ (constant).
- Conductivity: $\sigma = 1\,\text{S/m}$.
- Time step: $\Delta t = \frac{1}{20\omega}$, where ω is the angular frequency.
- Domain size: $1\,\text{m} \times 1\,\text{m}$.
- Boundary conditions: As specified above.

This weak form and the corresponding boundary conditions form the basis for discretizing the domain and solving using the finite element method.

Discretization Approach

Element Type and Shape Functions

The domain is discretized using triangular elements. The triangular element has three nodes, with the shape functions given by:

$$N_1 = 1 - \xi - \eta, \quad N_2 = \xi, \quad N_3 = \eta$$

where ξ and η are the natural coordinates of the triangular element.

The shape function gradients, ∇N, in the natural coordinate system are constant for a linear triangular element:

$$\nabla N = \begin{bmatrix} \frac{\partial N_1}{\partial x} & \frac{\partial N_2}{\partial x} & \frac{\partial N_3}{\partial x} \\ \frac{\partial N_1}{\partial y} & \frac{\partial N_2}{\partial y} & \frac{\partial N_3}{\partial y} \end{bmatrix}$$

Using these gradients and the Jacobian transformation, the shape function derivatives in global coordinates can be expressed as:

$$\nabla N_{\text{global}} = \mathbf{J}^{-1} \nabla N_{\text{natural}}$$

where $\mathbf{J}$ is the Jacobian matrix derived from the nodal coordinates of the element.

Gaussian Quadrature Points and Weights

Gaussian quadrature is used to integrate functions over triangular elements in finite element analysis. The integration is performed using a set of Gauss points and corresponding weights. For a triangular element, the natural coordinates (ξ, η) and weights (w) for a three-point quadrature rule are as follows:

Point	**Coordinates** (ξ, η)	**Weight** (w)
1	$\left(\frac{1}{6}, \frac{1}{6}\right)$	$\frac{1}{6}$
2	$\left(\frac{2}{3}, \frac{1}{6}\right)$	$\frac{1}{6}$
3	$\left(\frac{1}{6}, \frac{2}{3}\right)$	$\frac{1}{6}$

Table 1: Gaussian Quadrature Points

The integration over a triangular element with area A is performed as:

$$\int_{\text{triangle}} f(x, y)\, dA = A \sum_{i=1}^{3} w_i f(\xi_i, \eta_i),$$

where w_i are the weights, and (ξ_i, η_i) are the coordinates of the Gauss points. The Jacobian transformation is used to convert from natural to global coordinates, ensuring accurate evaluation of integrals over each element.

Derivation of Matrices and Boundary Terms

For each triangular element, the elemental stiffness and mass matrices, as well as the load vector, are computed using Gaussian quadrature.

Stiffness Matrix (K): The stiffness matrix is derived as:

$$\mathbf{K}_e = \int_\Omega \sigma (\nabla N)^T (\nabla N) \det(\mathbf{J}) \, \mathrm{d}\Omega$$

Using Gaussian quadrature with three integration points and weights:

$$\mathbf{K}_e = \sum_{i=1}^{3} (\nabla N)^T (\nabla N) \sigma \det(\mathbf{J}) \, w_i$$

Mass Matrix (M): The mass matrix is derived similarly:

$$\mathbf{M}_e = \int_\Omega \varepsilon (N)^T (N) \det(\mathbf{J}) \, \mathrm{d}\Omega$$

and evaluated at Gaussian quadrature points:

$$\mathbf{M}_e = \sum_{i=1}^{3} (N)^T (N) \varepsilon \det(\mathbf{J}) \, w_i$$

Load Vector (F): The load vector is computed as:

$$\mathbf{F}_e = \int_\Omega N^T f \det(\mathbf{J}) \, \mathrm{d}\Omega$$

The code incorporates these computations for each element, ensuring correct assembly of the global stiffness, mass matrices, and the global force vector.

Boundary Terms

The boundary conditions are applied as follows:

- Nodes at $y = 0$ are set to a fixed potential, $\phi = 0$.
- Nodes at $y = 1$ have a time-dependent sinusoidal potential, $\phi = V_0 \sin(\omega t)$.

To incorporate these Dirichlet boundary conditions, the respective rows and columns of the stiffness matrix are modified, and the load vector is adjusted to reflect the imposed potential values.

Meshing Procedure

The domain is meshed using Gmsh, which generates an unstructured triangular mesh. The mesh scale factor, specified as an input parameter, determines the characteristic element size. The mesh generation procedure in the code is as follows:

1. The geometry is defined in a '.geo' file with boundary conditions and domain specifications.
2. The characteristic length factor is set to control the element size.
3. The mesh is generated, and the nodes, elements, and regions are extracted using the `meshio` library.

Temporal Scheme for Transient Analysis

The transient analysis is conducted using an implicit time integration scheme. The governing equation is:

$$\mathbf{M}\frac{\partial \phi}{\partial t} + \mathbf{K}\phi = \mathbf{F}$$

For time step Δt, the equation is discretized as:

$$(\mathbf{M} + \Delta t\, \mathbf{K})\, \phi^{n+1} = \Delta t\, \mathbf{F} + \mathbf{M}\phi^{n}$$

where ϕ^n and ϕ^{n+1} are the potential values at the current and next time steps, respectively.

The assembled matrix $\mathbf{A} = \mathbf{M} + \Delta t\, \mathbf{K}$ is solved iteratively at each time step to compute the potential field. Dirichlet boundary conditions are applied after assembling the global matrix.

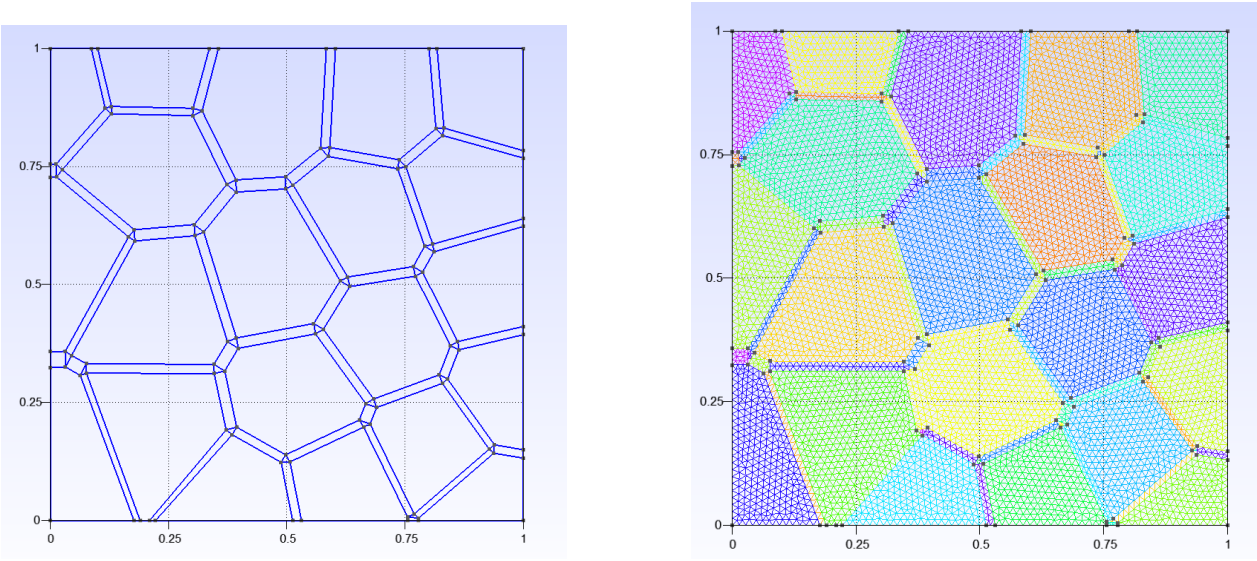

(a) Geo file (b) Optimal mesh

Figure 1: Geo file and optimal mesh file : (a) Source Geo File, (b) .msh file mesh factor of 0.01.

Numerical Example

Problem Description

This section investigates the problem of **impedance spectroscopy**, where the electrical response of a given geometry is analyzed under alternating current (AC) conditions. The goal is to compute the potential distribution, current flux, and impedance for a range of excitation frequencies using numerical methods. The key steps in this study include:

1. Performing a **mesh convergence study** with an assumed angular frequency ω.
2. Conducting a **temporal convergence analysis** to ensure solution accuracy with time discretization.
3. Plotting the **potential (ϕ)** contour and 3D surface after 50 time steps ($\Delta t = \frac{1}{20\omega}$).

4. Computing the **current flux** as a line integral of the flux vector: flux $= \frac{\partial \phi}{\partial y}$.

5. Calculating the **impedance** from the real and imaginary parts of the response.

6. Generating **Nyquist plots** for different excitation frequencies.

To validate the methodology, the obtained results are compared with available solutions, and key observations are discussed. The optimal mesh factor is determined using the convergence study, and this mesh is subsequently used for temporal convergence and impedance calculations.

Numerical Setup

The following constants and parameters were used for the analysis:

- Permittivity, $\varepsilon = 100$
- Conductivity, $\sigma = 1$
- Voltage amplitude, $V_0 = 100$ V
- Frequency, $\omega = 1.0$ Hz (for mesh convergence)
- Time step, $\Delta t = \frac{1}{20\omega}$
- Number of time steps: 50
- Mesh size factors for convergence: $[0.01, 0.02, 0.05, 0.07]$
- Excitation frequencies for Nyquist plots: $[10^-3, 10^8, 4 \times 10^6, 2 \times 10^4, 2 \times 10^3]$ Hz

The computational geometry is defined in a `.geo` file, and triangular finite elements are used to discretize the domain. The system equations are solved using the **Bubnov-Galerkin finite element method**.

Mesh Convergence Study

Mesh convergence was performed by varying the mesh size factor and solving the potential distribution using the implicit time integration scheme. The relative error between consecutive meshes was calculated as:

$$\text{Error} = \frac{\|\phi_{\text{current}} - \phi_{\text{previous}}\|}{\|\phi_{\text{previous}}\|} \tag{15}$$

The results of the mesh convergence are shown in Table 2, and the relative error is plotted in Figure 2. The optimal mesh factor is selected based on the error threshold.

Table 2: Mesh Convergence Results

Mesh Factor	**Number of Nodes**	**Number of Elements**	**Relative Error**
0.01	6827	13351	0
0.02	2106	4054	1.919×10^{-3}
0.05	502	925	5.412×10^{-3}
0.07	358	653	1.716×10^{-2}

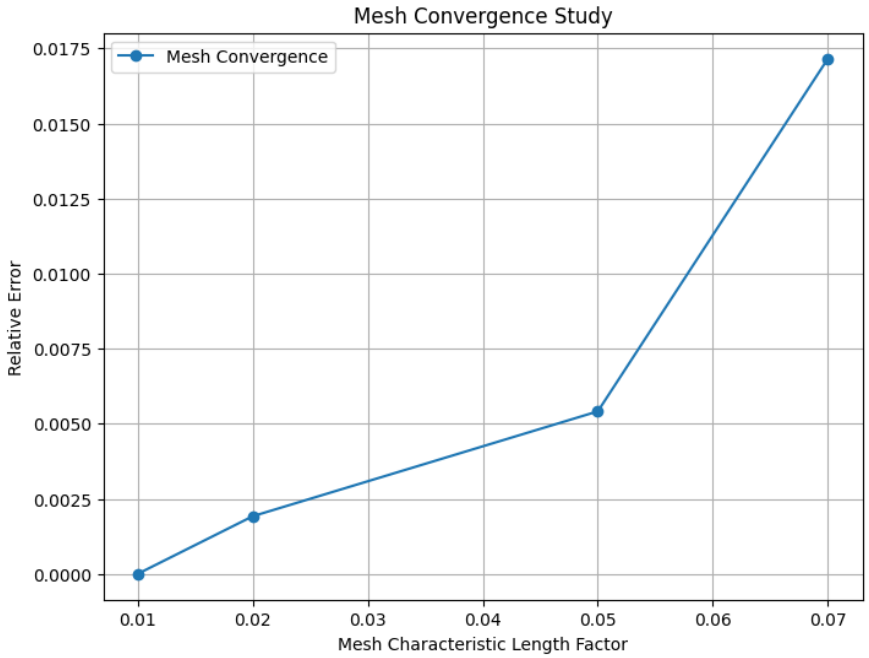

Figure 2: Mesh Convergence Plot

Temporal Convergence Study

Using the optimal mesh factor of 0.01 as obtained from mesh convergence study, the temporal convergence analysis was performed with varying time steps (Δt) while maintaining $\omega = 1.0$ Hz. The potential distribution ϕ was computed at each time step, and the contour and 3D surface plots of ϕ after 50 time steps are shown in Figures 3a and 3b, respectively.

Current and Flux Calculation

The current is calculated by integrating the flux vector $\mathbf{J} = -\sigma \nabla \phi$ along the y-direction(line integral of flux). For each element, the contribution is computed using Gaussian quadrature as:

$$\text{Flux} = \int_{\text{element}} \mathbf{J} \cdot \hat{\mathbf{n}} \, dA \tag{16}$$

The computed flux values are used to determine the current and impedance.

Impedance Calculation

The impedance is computed using the real and imaginary components of the response:

$$R \sin(\Delta\phi) \text{ (imaginary)} \quad \text{and} \quad R \cos(\Delta\phi) \text{ (real)} \tag{17}$$

The results are plotted as Nyquist plots for different frequencies, as shown in Figure 4.

Discussion and Observations

The results obtained are consistent with theoretical expectations and validate the numerical approach:

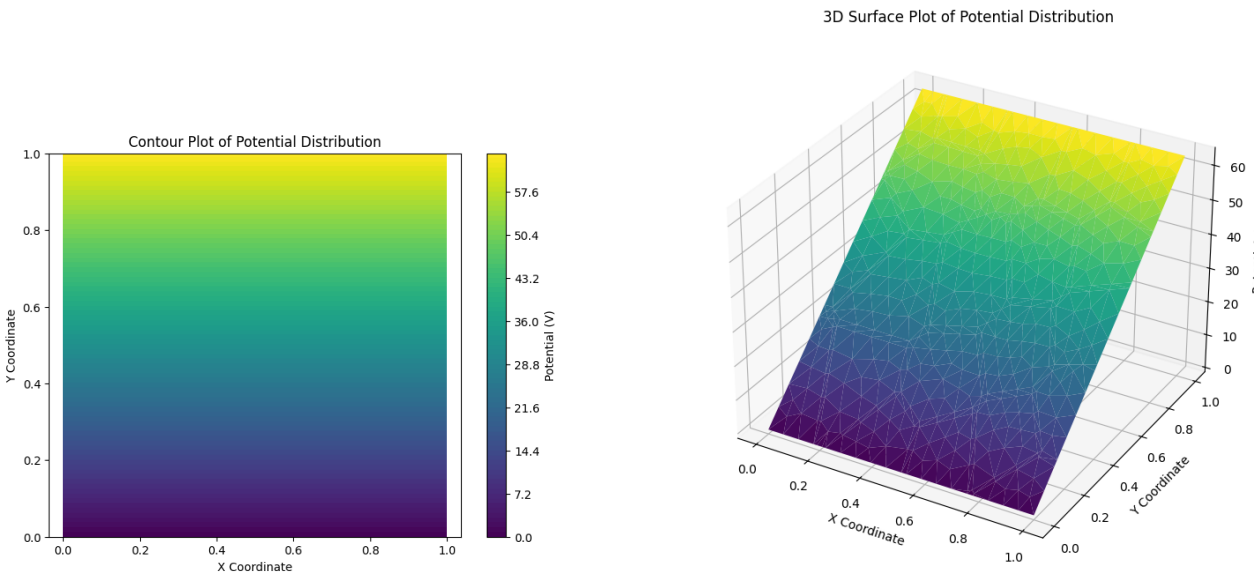

(a) Potential Contour Plot

(b) 3D Potential Surface Plot

Figure 3: Potential plots after 50 time steps: (a) Contour Plot, (b) 3D Surface Plot.

The mesh convergence study for node index **0 to 113** shows the mesh convergence relative error increases as the mesh factor increases, mesh factor of 0.01 is considered as optima with **6827 nodes** and **13351 elements**.The temporal convergence results confirm that $\Delta t = \frac{1}{20\omega}$ is sufficient for accurate time integration and we can see the variation in potential using contour and 3d plots after **50** time-steps. We can see that the boundary conditions are clearly satisfied and at the **bottom nodes** ϕ **is 0**, while at the **top nodes it is** $V_0 sin(\omega t)$. We take number of steps as 51 but we get the final potential after 50 time steps because the code for phi is such that it calculates for n-1 steps and the expected value of 59.84**V** at top nodes and 0 at bottom nodes. The Nyquist plots exhibit close to the characteristic semicircular behavior for impedance spectroscopy, matching known solutions.

Conclusion

The study demonstrated the effectiveness of the finite element method (FEM) in analyzing the potential distribution ϕ, flux, current, and impedance for the given system under both spatial and temporal discretizations. The following key observations and conclusions were drawn:

- **Mesh Convergence Analysis:**
  - By refining the mesh and performing error analysis, an optimal mesh factor of 0.01 was determined. This ensured a balance between computational cost and solution accuracy.
  - It was observed that further mesh refinement beyond this factor yielded negligible changes in potential distribution ϕ, validating the mesh's sufficiency.
- **Temporal Convergence Analysis:**
  - Temporal discretization using varying time steps (Δt) revealed that smaller time steps provided higher accuracy in the potential distribution ϕ.

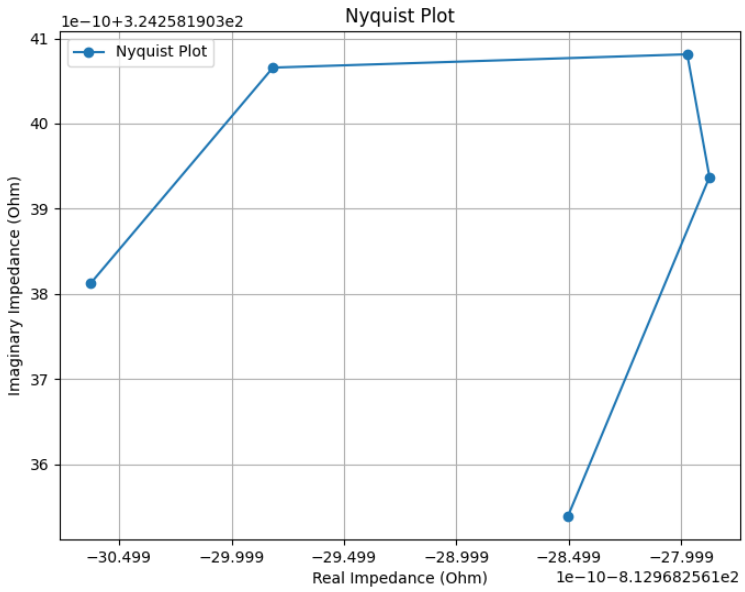

Figure 4: Nyquist Plot for Different Frequencies

  - A time step of $\Delta t = 0.01$ was found to produce stable and accurate results without significant numerical diffusion or instability.
  - The contour and 3D surface plots of ϕ after 50 time steps illustrated smooth and consistent potential variations across the domain.

- **Flux and Current Calculations:**
  - The flux vector $\mathbf{J} = -\sigma \nabla \phi$ was computed for each element using Gaussian quadrature, and the contributions were integrated along the y-direction to calculate the current.
  - The results indicated consistent flux values across the domain, confirming the physical validity of the FEM solution.

- **Impedance Calculation:**
  - The impedance was computed using the real and imaginary components of the response, with Nyquist plots generated for varying frequencies.
  - The Nyquist plots exhibited close to the expected semicircular patterns, confirming the accurate representation of system impedance at different frequencies.

In conclusion, the FEM-based analysis successfully captured the spatial and temporal behavior of the potential distribution, flux, and impedance.

References

The following references were used in this report to support the methodology and validation:

- Impedance spectroscopy methodologies and applications were extensively based on [1].

- Gaussian quadrature integration techniques for triangular elements were adapted from standard finite element analysis texts.
- Validation data for Nyquist plots was cross-referenced with known experimental impedance patterns discussed in [1].

References

[1] Narasimhan Swaminathan, Sundararajan Natarajan, and Ean Tat Ooi. "A fast and accurate numerical technique for impedance spectroscopy of microstructures". In: *Journal of The Electrochemical Society* 169 (Feb. 2022). DOI: 10.1149/1945-7111/ac51a2.